International Journal of Energy Research

WILEY

RESEARCH ARTICLE OPEN ACCESS

Optimizing Building Energy Systems Using Generalized Disjunctive Programming: Improving Model Precision and Decision-Making Efficiency

Yi Nie | Thomas Schreiber | Dirk Müller

RWTH Aachen University, E.ON Energy Research Center, Institute for Energy Efficient Buildings and Indoor Climate, Mathieustr. 10, Aachen, Germany

Correspondence: Yi Nie (yi.nie@rwth-aachen.de)

Received: 17 December 2024 | **Revised:** 25 December 2025 | **Accepted:** 24 January 2026

Academic Editor: Rajashik Paul

Keywords: building energy systems | generalized disjunctive programming | part load operation | price model | subsidy

ABSTRACT

This paper examines the optimization of building energy systems (BESs) through the lens of generalized disjunctive programming (GDP), a methodology that streamlines the modeling of intricate logical structures and discrete decisions. The study concentrates on three pivotal aspects of BES optimization: the imposition of minimum part-load constraints, the selection of discrete equipment sizes and pricing, and the integration of subsidy policies. These elements are of critical importance due to the operational limitations of real-world technologies, the necessity for precise equipment investment strategies, and the significant influence of policy incentives on system design. The results of comprehensive case studies demonstrate the significant impact of these constraints on decision-making and system performance. Specifically, part-load constraints result in a shift in the operational priorities of equipment, with an increased reliance on energy storage systems, particularly during periods of low demand. Additionally, pricing models have a significant impact on equipment selection, while subsidy integration has the effect of reducing overall costs and encouraging the adoption of energy-efficient technologies, such as heat pumps. However, the adoption of GDP introduces computational challenges, particularly due to the complex disjunctive constraints applied across multiple time steps, which require careful consideration in BES optimization.

1 | Introduction

1.1 | Background

In Europe, energy consumption by buildings accounts for 29.6% of the total final energy consumption, thereby underscoring a significant impact on the overall energy landscape [1]. Research indicates that there is considerable potential for annual energy savings through integrated system optimization within buildings [2]. A plethora of energy system tools have been developed and employed extensively, assisting in the design and operation optimization of building energy systems (BESs) while offering economically viable solutions to system designers [3, 4].

Mixed-integer linear programming (MILP) is a prevalent methodology employed in comprehensive BES optimization models, particularly in addressing constraints such as minimum part-load limitations, part-load efficiencies, and start-up costs [5]. These features are of critical importance in BESs, where discrete decisions and operational constraints are commonplace. However, modeling these features typically necessitates the utilization of the big-M method, which involves the incorporation of binary variables and a big-M constant for the reformulation of constraints. Although this approach is effective, it can significantly increase the complexity and computational cost of the model.

For more complex control systems or conditional constraints, manually constructing MILP models using the big-M method is feasible, but often cumbersome and time-consuming. Furthermore, while MILP is capable of handling logical relationships, it often struggles to efficiently manage complex logical expressions that are essential for complying with policy-driven subsidies and regulatory frameworks.

Generalized disjunctive programming (GDP), originally introduced by Raman and Grossmann [6], offers a means of simplifying the modeling of complex logical relationships, such as disjunction conditions, where only one of the several possible scenarios or constraints must be satisfied. These relationships are often represented as "either–or" decisions. The capabilities of MILP are extended by GDP, which represents the complex, nonlinear, and discrete behaviors inherent in BESs in a more effective manner. GDP models can be reformulated into MILP problems using a variety of mathematical techniques, with the big-M and convex hull reformulation methods being the most prevalent [7]. The effectiveness of these mathematical techniques is contingent upon the particular context of application.

Incorporating GDP into the MILP framework permits a more comprehensive consideration of the various factors involved in the design and optimization of BESs. These factors include technical, economic, and regulatory aspects. It markedly enhances the precision of the optimization models and the performance of decision-making processes. This integrated framework allows for a more comprehensive approach to the design of BESs, aligning with the broader goals of energy efficiency and sustainability in today's dynamic policy landscape.

1.2 | Current Research on BESs Modeling with MILP

The MILP approach has been widely adopted for optimizing BESs, demonstrating its versatility in design and operational optimization across a range of building types. This encompasses applications in individual residential and nonresidential buildings, as well as multibuilding complexes, thereby illustrating the extensive applicability of MILP in energy system design. Lindberg et al. [8] employed MILP to attain the optimal energy balance in a German multifamily residence, effectively minimizing costs while adhering to zero energy building standards. Lozano et al. [9] optimized the combined heat, cooling, and power system in a hospital with the objective of determining the optimal sizes of the various equipment components, thereby ensuring efficient operation and energy management. Iturriaga et al. [10] present an urban project in which multiple buildings are considered as a single entity in order to meet specific non-renewable primary energy consumption targets.

Moreover, the flexibility of MILP extends to encompass a range of technological equipment. Wouters et al. [11] investigate the integration of small-scale wind turbines, absorption chillers, and battery banks in an Australian residential neighborhood, aiming to optimize energy distribution and utilization. Alvarado et al. [12] assess the impact of different technology scenarios, including combined heat and power and organic Rankine cycle, on system performance through the lens of MILP. Kuang et al. [13] conduct an optimization of photovoltaic panels in a building and the electric vehicle charging station, with the objective of significantly reducing the operational costs for both the building and the charging station.

In addition to optimizing the energy supply systems of buildings, research has also focused on the potential for optimizing building envelopes. In their study, Schütz et al. [14] considered both the design of energy conversion units and building envelopes for residential buildings. A linear equation was employed to model the thermal mass and heat transfer coefficients of the building, integrating both aspects into a unified model to identify an optimal solution [14]. Similarly, Iturriaga et al. [15] examined both energy supply systems and energy-saving measures on envelopes. In this instance, however, the energy-saving measures were treated as a separate model, with no direct modeling of the heat exchange processes of the building envelope [15].

Specific technical features and environmental benefits are also within the purview of MILP. For example, Steen et al. [16] employed MILP to model multilayer thermal energy storage systems, thereby enhancing the accuracy of loss tracking. Similarly, Rossi et al. [17] utilized MILP in conjunction with life cycle assessment to optimize designs for both economic and environmental gains. The extensive application of MILP in BESs optimization demonstrates its versatility and adaptability across various building types and complex systems.

1.3 | Current Research on Optimization Model with GDP

GDP represents an alternative modeling approach to algebraic mixed-integer programming. The approach involves the specification of Boolean and continuous variables in algebraic constraints, disjunctions, and logic propositions. This approach not only streamlines the development of models by making the formulation process intuitive, but it also retains the underlying logic structure of the problem within the model, which can be exploited to find solutions more efficiently [7]. The versatility of GDP is evident across a spectrum of applications, including chemical processing, energy systems, and industrial production planning.

Notably, GDP has been applied in the chemical and process engineering domain. Jackson and Grossmann [18] employ GDP to optimize the design of a reactive distillation column, with a particular focus on the identification of optimal plate numbers, feed locations, and operations of condensers and boilers. The objective is to minimize both the annualized investment costs and the operational costs [18]. Similarly, Yeomans and Grossmann [19] employ GDP for synthesizing distillation sequences, where the disjoint solution spaces and logical connectivity present inherent challenges. In related applications, Onishi et al. [20] discuss the use of GDP in process systems engineering for oil refineries and cryogenic technologies, optimizing steam distribution according to energy demands and operational conditions. This is complemented by Onishi et al.'s [21] work on retrofitting heat exchanger networks in liquefied natural gas production processes, where GDP facilitates enhanced energy integration.

In the field of building energy, GDP is primarily utilized for the optimization of control systems, particularly model predictive control (MPC). Bhattacharya et al. [22] put forth a GDP–based MPC model for piecewise-affine systems with implicit switching logic

and well-suited for implementation in a multitude of hybrid systems with intricate logic rules. Kim et al. [23] apply GDP in an MPC system to coordinate the operations of chillers, water tanks, and solar farms within power grids. Moreover, Cho et al. [24] employ GDP in their study on long-term expansion planning of power generation systems, utilizing it to optimize investment decisions and operational strategies, thereby enhancing system reliability. Stewart et al. [25] integrate GDP with differential-algebraic equations and stochastic simulation for the optimization of emergency control in power grids under fault conditions.

Additionally, in industrial and production domains, GDP is employed to optimize product design. Manassaldi et al.'s [26] research on the design of air-cooled heat exchangers uses GDP to select components and configurations, such as finned tubes, flow regimens, and heat transfer coefficients, ensuring optimal design through the use of logic propositions that relate various system aspects.

1.4 | Contributions

This research makes several significant contributions to the field of BESs design optimization. First, it unifies GDP and MILP within a single framework, thereby enhancing MILP models with the broader capabilities of GDP. This integration permits the more intricate and dynamic management of practical operational conditions in energy management scenarios. Second, the research offers a conceptual illustration of the potential performance of the integrated model. The theoretical analysis and illustrative examples presented across multiple scenarios demonstrate how GDP can significantly enhance decision-making under variable conditions influenced by external factors, such as policy changes. Furthermore, this study presents a comparative analysis of two mathematical approaches, namely, the big-M method and convex hull reformulation, for the reformulation of GDP models. It elucidates the respective advantages of these approaches in different contexts. Finally, the code and evaluation scenarios are accessible on GitHub (https://github.com/RWTH-EBC/BESDOT).

1.5 | Paper Organization

The rest of the paper is divided into four main sections. Section 2 describes the methodologies used in this study, covering both MILP and GDP model formulations. Section 3 applies these methodologies to a reference case and six extended use cases, demonstrating their implementation and effectiveness. Section 4 analyzes the results of the case studies and discusses their implications for BESs. Section 5 provides a critical evaluation of the results, highlighting limitations, practical applications, and potential improvements to the models. Finally, Section 6 summarizes the key findings and explores potential directions for future research.

2 | Research Method

Section 2 presents the formulation of the model used in this study, which aims to determine the optimal size and operational status of energy system devices while evaluating economic parameters. The model operates on an annual basis and processes data at hourly intervals, allowing for detailed and dynamic simulation of energy systems throughout the year. To speed up the computational process, the study uses a temporal hierarchical clustering method that reduces the 365 days and 8760 h of the full year to 16 representative days with a total of 384 h. The model was implemented in Python 3.9.12 using Pyomo 6.4.2 [27] and solved with Gurobi Optimizer 9.0.0 (win64) [28] via the Pyomo–Gurobi interface. Computations were performed on a desktop computer equipped with an Intel(R) Core(TM) i7-10700 CPU (8 cores, 2.90 GHz) and 32 GB of RAM, running Windows 10. Unless otherwise noted, all runs were executed in single-threaded mode.

2.1 | MILP Model Formulation

This MILP model optimizes economic efficiency by balancing capital costs, operational costs, and potential revenue from energy sales, while adhering to all relevant operational constraints. Sections 2.1.1 and 2.1.2 detail the objective function and constraints inherent in the model.

2.1.1 | Objective Function

The objective function seeks to minimize the total annualized cost, C_{tot}, which includes the annualized investment ($\text{a}_d \cdot C_{\text{inv},d}$) for each device d, the operational costs ($C_{\text{op},t,e}$) for each type of energy e consumed over the time periods t, and subtracting the revenue from electricity fed back into the grid during the same periods ($R_{\text{feed},t}$). The annualization factor a_d is applied to the investment ($C_{\text{inv},d}$) to reflect the distribution of these costs over the expected life of the devices.

$$\text{minimize } C_{\text{tot}} = \sum_{d \in D} \text{a}_d \cdot C_{\text{inv},d} + \sum_{t \in T} \sum_{e \in E} C_{\text{op},t,e} - \sum_{t \in T} R_{\text{feed},t}. \tag{1}$$

2.1.2 | Model Constraints

The developed model uses an object-oriented programming framework, in which generic MILP constraints are defined across multiple superclasses. These constraints are fundamentally based on linear equations, which serve as the core building blocks of the optimization model. This modular and extensible structure encapsulates the primary generic constraints in Equations (2)–(9) within these superclasses. Detailed MILP constraints specific to each device are described in the aforementioned GitHub repository.

2.1.2.1 | Capacity Constraints. The capacity constraints ensure that the energy output of each device d at each time step t does not exceed its rated capacity ($P_{\text{rated},d}$).

$$P_{\text{out},d,t} \leq P_{\text{rated},d} \; \forall d \in D, \forall t \in T. \tag{2}$$

In the baseline MILP formulation, devices without explicit minimum part-load requirements are modeled with continuous outputs and no generic on/off binaries. Under a cost-minimization objective with nonnegative marginal operating costs, any unnecessary output is penalized, and hence, the optimizer sets $P_{\text{out},d,t} = 0$ whenever the device is not needed. Introducing generic binaries $y_{d,t}$ for all devices would increase problem size without affecting optimal decisions in this baseline setting.

2.1.2.2 | Investment Constraints. These constraints establish a direct proportionality between the rated capacity of the device ($P_{\text{rated},d}$) and its corresponding investment cost ($C_{\text{inv},d}$). In this context, $c_{\text{unit},d}$ represents the cost per unit of power, which is assumed to be constant. The formula indicates that increasing the capacity of the device will linearly increase the investment cost, assuming a constant cost per unit of power.

$$C_{\text{inv},d} = P_{\text{rated},d} \cdot c_{\text{unit},d}. \tag{3}$$

2.1.2.3 | Conversion Constraints. The relationship between energy output and input is defined by the device's efficiency ($\eta_{d,t}$). For air source heat pumps, this efficiency is further influenced by the coefficient of performance, which fluctuates throughout the year due to varying air temperatures.

$$P_{\text{out},d,t} = \eta_{d,t} \cdot P_{\text{in},d,t} \; \forall d \in D, \forall t \in T. \tag{4}$$

2.1.2.4 | Storage Constraints. This equation models the energy storage process for each time step t, except the last one. Here, $E_{\text{stored},t}$ represents the energy stored at time t, η_{self} is the self-discharge rate of the storage system, η_{in} is the efficiency of charging the storage, and η_{out} is the efficiency of discharging the storage. This formulation accounts for energy input, output, and self-discharge losses within each time step.

$$\begin{aligned} E_{\text{stored},t+1} = {} & E_{\text{stored},t} \cdot (1 - \eta_{\text{self}}) + P_{\text{in},t} \\ & \cdot \eta_{\text{in}} - P_{\text{out},t}/\eta_{\text{out}} \; \forall t \in T \setminus \{t_{\text{last}}\}. \end{aligned} \tag{5}$$

In models where time series data are aggregated using clustering methods to represent typical days, it is important to ensure the continuity of energy storage between these representative periods. When transitioning from one typical day to the next, differences in the weighting of these days can lead to unrealistic jumps in stored energy levels if not properly accounted for. To address this issue, a constraint is included that adjusts the stored energy at the end of each typical day by taking into account the weight assigned to that day, as well as the efficiency and loss factors associated with energy storage. This approach is expressed mathematically as follows:

$$\begin{aligned} \sum_{i=1}^{N} \left(E_{\text{stored},i\cdot\tau} \cdot (1 - \eta_{\text{self}}) + P_{\text{in},i\cdot\tau} \cdot \eta_{\text{in}} - \frac{P_{\text{out},i\cdot\tau}}{\eta_{\text{out}}} \right) \\ \cdot w_i = \sum_{i=1}^{N} E_{\text{stored},(i-1)\cdot\tau+1} \cdot w_i. \end{aligned} \tag{6}$$

In this formulation, $E_{\text{stored},i\cdot\tau}$ represents the energy stored at the last time step of the ith typical day, while $E_{\text{stored},(i-1)\cdot\tau+1}$ represents the energy stored at the first time step of the ith typical day, adjusted for self-discharge losses η_{self}. $P_{\text{in},i\cdot\tau}$ and $P_{\text{out},i\cdot\tau}$ denote the energy input and output at the end of the ith typical day, each adjusted by their respective efficiencies η_{in} and η_{out}. The term w_i is the weight of the ith typical day, τ is the time step within a typical day, set to 24 h, and N is the total number of typical days. This constraint is necessary to accurately model systems that use representative days and to prevent any unintended energy accumulation or deficit within the system.

To maintain cyclic continuity in the energy storage system, an additional constraint is applied.

$$E_{\text{stored},1} = E_{\text{stored},t} \cdot (1 - \eta_{\text{self}}) + P_{\text{in},t} \cdot \eta_{\text{in}} - P_{\text{out},t}/\eta_{\text{out}} \text{ for } t = t_{\text{last}}. \tag{7}$$

This equation ensures that the energy stored at the end of the considered period (at t_{last}) is equal to the energy stored at the beginning (at $t = 1$).

2.1.2.5 | Energy Balance Constraints. Here, δ_{jd} represents the connection between device j and device d. If $\delta_{jd} = 1$, energy flows from device j to device d; if $\delta_{jd} = 0$, there is no energy flow from device j to device d. This ensures energy balance within the system at each time step.

$$P_{\text{in},d,t} = \sum_{j \in D} \delta_{jd} P_{j,d,t} \; \forall d \in D, \forall t \in T. \tag{8}$$

These connection indicators, δ_{jd}, are stored in a matrix that represents all allowed energy flows within the system. For example, Figure 1 illustrates the interconnection topology between three devices, and this topology can be mathematically represented in a matrix as shown in Table 1.

Similarly, for the energy flowing out of a device is subject to the following constraint.

$$P_{\text{out},d,t} = \sum_{j \in D} \delta_{dj} P_{d,j,t} \; \forall d \in D, \forall t \in T. \tag{9}$$

2.1.2.6 | Note on Ramping Constraints. Ramping-up or ramping-down constraints, often included in unit commitment

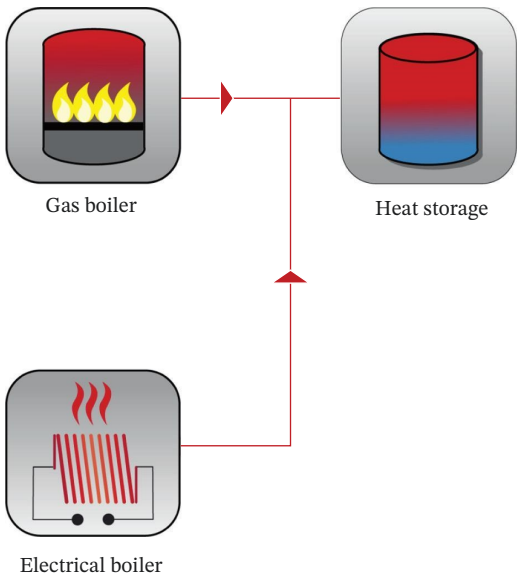

FIGURE 1 | Example of connection topology.

TABLE 1 | Example of connection topology in matrix form.

δ_{jd} (j in rows, d in columns)	Gas boiler	Electrical boiler	Heat storage
Gas boiler	0	0	1
Electrical boiler	0	0	1
Heat storage	0	0	0

or power system optimization, are not part of the present formulation. In this study, the 1-h time resolution and the types of devices considered (boilers and heat pumps) render such constraints unnecessary, since these units can typically adjust within 1 h. The framework can, however, be extended to include ramping constraints if equipment with stricter dynamics is modeled.

2.2 | GDP Model Formulation

The GDP model extends the capabilities of traditional MILP models by incorporating logical propositions and disjunctive constraints. Its mathematical formulation is as follows [23]:

$$\begin{aligned} &\text{minimize} && f(x) && \text{(Objective function)} \\ &\text{subject to} && g(x) \le 0 && \text{(Algebraic constraints)} \\ & && \bigvee_{m \in M} \begin{bmatrix} Y_{mn} \\ r_{mn}(x) \le 0 \end{bmatrix} && \text{(Disjunctions)} \\ & && \Omega(Y) = \text{True} && \text{(Logic propositions)} \\ & && \text{L} \le x \le \text{U} && \text{(Continuous variables)} \\ & && Y_{mn} \in \{\text{True, False}\} && \text{(Boolean variables)} \end{aligned} \tag{10}$$

The model contains disjunctions indexed by $m \in M$, where each disjunction contains terms indexed by $n \in N_m$, which are linked together by an OR operator ($\vee$). Each disjunctive term is associated with a Boolean variable Y_{mn} and a set of inequalities $r_{mn}(x) \le 0$. Only one Boolean variable can be true within each disjunction. If a disjunctive term is selected ($Y_{mn} = \text{True}$), the corresponding inequalities $r_{mn}(x) \le 0$ are enforced; otherwise, the constraints are ignored. The logical relations between the Boolean variables are represented by logical propositions $\Omega(Y) = \text{True}$.

To ensure that the Boolean variables in the disjunctive formulations represent mutually exclusive choices rather than a simple logical OR, an additional exclusivity constraint is included. In logic-based optimization, exclusivity is commonly denoted by an underlined disjunction symbol. In this work, the operator $\veebar$ is used to denote binary exclusive OR between two Boolean variables, and $\bigvee$ is used to denote the exclusive OR across a finite set of Boolean variables. Equations (11)–(13) and (15), the additional line explicitly enforces that exactly one of the Boolean variables is true in each disjunction.

2.2.1 | Modeling of Part Load Operation With GDP

The GDP model can be used to more accurately simulate the operational states of energy system components, such as minimum part load operation. Many devices have a specified minimum part load ratio. For example, gas boilers experience significant energy losses when operating below 40% part load [29]. Some manufacturers specify a minimum part load ratio between 15% and 30% for their products. The part load operating constraint can be modeled as follows:

$$\begin{aligned} &\begin{bmatrix} Y_{d,t,\text{on}} \\ P_{\text{out},d,t} \ge \alpha_d \cdot P_{\text{rated},d} \end{bmatrix} \bigvee \begin{bmatrix} Y_{d,t,\text{off}} \\ P_{\text{out},d,t} = 0 \end{bmatrix} \forall t \in T, \\ &Y_{d,t,\text{on}} \veebar Y_{d,t,\text{off}} = \text{True}. \end{aligned} \tag{11}$$

where α_d is the minimum part load ratio for the device d. The Boolean variable $Y_{d,t,\text{on}}$ indicates whether the device is operating and $Y_{d,t,\text{off}}$ indicates whether the device is not operating. The disjunction ensures that at any time t and the device d is either operating above its minimum part load ratio or is completely turned off.

2.2.2 | Modeling of Variable Specific Device Prices With GDP

In BESs, accurate device pricing modeling is critical for effective financial planning and operational optimization. Typically, specific price modeling without a fixed base price for linear models is a common approach. However, this method can lead to biases in device selection due to its simplicity and potential mismatch with actual market prices.

In addition to the simple specific price approach, two additional methods have been explored with the use of GDP in order to do price modeling more effectively:

- The first method incorporates a fixed base price in addition to the specific price, which helps to better align the model prices with real-world cost structures, especially for smaller devices.
- The second method treats all feasible device options as discrete points, allowing for selection among actual products available in the market.

Figure 2 illustrates the differences between these three pricing models. For models that regress on a fixed base price, a simple linear relationship between total cost and device size can be defined. However, this approach may incorrectly suggest a non-zero cost for a size of zero because the regression line intersects the y-axis above zero. To address this, the fixed base price model is extended to ensure that the cost is set to zero when the device size is zero. This can be represented by the following disjunction:

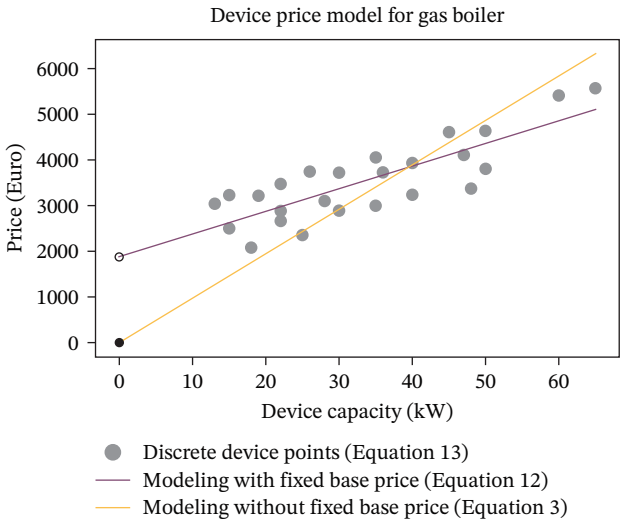

FIGURE 2 | Comparison of three different pricing models. The gray dots represent discrete pricing points, the purple line represents the model with a fixed base price, and the orange line represents the model that regresses through the origin.

$$\begin{bmatrix} Y_{d,\text{buy}} \\ C_{\text{inv},d} = P_{\text{rated},d} \cdot c'_{\text{unit},d} + F_d \\ P_{\text{rated},d} \geq P_{\min,d} \end{bmatrix} \bigvee \begin{bmatrix} Y_{d,\text{not}} \\ C_{\text{inv},d} = 0 \\ P_{\text{rated},d} = 0 \end{bmatrix}, \quad Y_{d,\text{buy}} \veebar Y_{d,\text{not}} = \text{True}. \tag{12}$$

In this formulation:

- $Y_{d,\text{buy}}$ is a Boolean variable that is true if the device is purchased.
- $C_{\text{inv},d}$ represents the investment cost of device d.
- $P_{\text{rated},d}$ is the rated power or capacity of device d.
- $c'_{\text{unit},d}$ represents the unit cost of the device per unit of capacity when using the regression model with a fixed base price.
- F_d is the fixed base price of the device.
- $P_{\min,d}$ is the minimum capacity threshold for the device.

In addition, when using GDP for modeling, the system can effectively handle discrete choices among available device options, which is critical for accurately capturing the complexity of real-world decision scenarios. Specifically, Section 2.2.2 introduces the third approach, where costs vary depending on the discrete sizes of the devices. In this context, k is the index representing the discrete options available for each device d. The disjunctions ensure that for each device d, only one discrete option is selected at a time: either a specific device option is selected, or no device is selected at all. This can be modeled using the following formulation:

$$\bigvee_{k \in K} \begin{bmatrix} Y_{d,k} \\ C_{\text{inv},d} = C_{\text{inv},k} \\ P_{\text{rated},d} = P_{\text{rated},k} \end{bmatrix} \bigvee \begin{bmatrix} Y_{d,\text{not}} \\ C_{\text{inv},d} = 0 \\ P_{\text{rated},d} = 0 \end{bmatrix}, \quad \bigvee \left(\{Y_{d,k}\}_{k \in K} \cup \{Y_{d,\text{not}}\} \right) = \text{True}. \tag{13}$$

In this formulation:

- $Y_{d,k}$ is a Boolean variable indicating the selection of device option k.
- $C_{\text{inv},k}$ represents the investment cost of device option k.
- $P_{\text{rated},k}$ is the rated power or capacity of device option k.
- $Y_{d,\text{not}}$ is a Boolean variable that is true if no device is selected.
- K is the set of all feasible discrete device options for device d.

This approach allows for flexible and accurate modeling of device pricing and selection based on discrete device sizes in the context of BESs.

2.2.3 | Modeling of Subsidy Policies

Subsidy policies can be effectively modeled using GDP to reflect different government incentives. The model developed considers two primary types of subsidies: purchase subsidies and operational subsidies. Purchase subsidies, which are typically related to the installed capacity of the device, can follow a tiered or linear structure. Operational subsidies, on the other hand, are allocated based on the amount of energy produced by the equipment. Section 2.2.3 introduces the modeling of purchase subsidies as an example; further details on operational and other types of subsidies considered in the case study (Tables A1–A3) can be found in the open source model repository.

Purchase subsidies can be categorized based on device capacity, investment amount, or surface area. The objective function needs to be adjusted to account for the subsidy amounts, which are annualized similarly to investments.

$$\text{minimize } C_{\text{tot}} = \sum_{d \in D} a_d \cdot C_{\text{inv},d} + \sum_{t \in T} \sum_{e \in E} C_{\text{op},t,e} - \sum_{t \in T} R_{\text{feed},t} - \sum_{d \in D} a_d \cdot S_{\text{purchase},d}, \tag{14}$$

where $S_{\text{purchase},d}$ is the purchase subsidy for the device d. Table 2 shows the tiered subsidy policy for photovoltaic installations in Düsseldorf.

The maximum subsidy for photovoltaic is limited to 10,000 Euros, if it reaches or exceeds the upper limit. The corresponding GDP formulation for such a tiered subsidy can be expressed as follows:

$$\begin{bmatrix} Y_{\text{PV,small}} \\ S_{\text{purchase,PV}} = P_{\text{rated,PV}} \cdot 300 \\ P_{\text{rated,PV}} \leq 10 \\ P_{\text{rated,PV}} \geq 0.6 \end{bmatrix} \bigvee \begin{bmatrix} Y_{\text{PV,medium}} \\ S_{\text{purchase,PV}} = 3000 + (P_{\text{rated,PV}} - 10) \cdot 200 \\ P_{\text{rated,PV}} \leq 45 \\ P_{\text{rated,PV}} \geq 10 \end{bmatrix} \bigvee \begin{bmatrix} Y_{\text{PV,large}} \\ S_{\text{purchase,PV}} = 10000 \\ P_{\text{rated,PV}} \geq 45 \end{bmatrix}, \quad Y_{\text{PV,small}} \veebar Y_{\text{PV,medium}} \veebar Y_{\text{PV,large}} = \text{True}. \tag{15}$$

In this formulation:

- $Y_{\text{PV,small}}$ is a Boolean variable indicating whether the photovoltaic capacity is in the low tier.
- $Y_{\text{PV,medium}}$ is a Boolean variable indicating whether the photovoltaic capacity is in the medium tier.
- $Y_{\text{PV,large}}$ is a Boolean variable indicating whether the photovoltaic capacity is in the large tier.
- $S_{\text{purchase,PV}}$ is the purchase subsidy for photovoltaic.
- $P_{\text{rated,PV}}$ is the rated capacity of the photovoltaic in kWp.

Operational subsidies, like purchase subsidies, can also be effectively modeled using GDP. This approach allows for the integration of both types of subsidies within a single project, recognizing that they are typically applicable concurrently. Where there are specific conditions between different subsidies, such as where the

TABLE 2 | Subsidy for photovoltaic installations based on capacity in Düsseldorf.

Capacity range (kWp)	Total subsidy amount
0.6–10 kWp	300 Euro per kWp
10–45 kWp	3000 Euro + 200 Euro per kWp above 10 kWp
≥ 45 kWp	10,000 Euro

application of one affects the eligibility or amount of the other, these relationships can be accurately represented using logical propositions.

When GDP disjunctions (e.g., minimum part load, discrete pricing, and tiered subsidies) are activated, their Boolean activations are mapped to binaries through the chosen GDP-to-MILP reformulation (Section 2.3), thereby introducing integrality only for those logical constructs.

2.3 | Reformulation Methods for GDP

GDP models can either be solved directly using dedicated algorithms (e.g., logic-based branch-and-bound) or, more commonly, through reformulation into MILP problems so that they can be handled by standard MILP solvers. The Pyomo framework, which was employed in this study, supports both approaches and provides an extensive implementation environment for GDP modeling [30]. In this work, the focus is placed on the two most widely used reformulation techniques, namely the big-M and the convex hull method. A general illustration of these reformulations, together with an example, is provided in Appendix A.

2.3.1 | Big-M Method

The big-M method is one of the most widely used techniques for converting logical constraints in GDP into MILP–compatible forms. By introducing a sufficiently large constant M, the method enables or disables specific constraints depending on the value of associated binary variables. This approach is straightforward and relatively easy to implement, making it a popular choice for many GDP problems. However, the method presents certain challenges: the choice of M is critical, as values that are too large or too small can lead to numerical instability or inefficient computation [31]. In addition, big-M formulations typically increase the number of binary variables and auxiliary constraints, thereby adding to the computational burden. For the big-M reformulation, the implementation relies on the default big-M transformation provided by Pyomo, which automatically infers suitable bounds from variable domains. Manual specification of M values was not required in this study.

2.3.2 | Convex Hull Method

The convex hull method provides an alternative reformulation that yields a tighter continuous relaxation compared to big-M [32]. It achieves this by introducing disaggregated variables and linking constraints, which more precisely represent the feasible region of the disjunction. While this tighter formulation can improve solution quality and solver performance in some cases, it usually results in a larger MILP due to the additional variables and constraints and may require more computational resources in terms of memory and presolve time [33]. In practice, the choice between big-M and convex hull depends on the trade-off between tighter relaxations and the overhead of increased problem size.

3 | Case Study

Section 3 presents a series of case studies designed to evaluate the integration of GDP models into BES optimization. The initial scenario, referred to as the reference case, is constructed using only the MILP model introduced in Section 2.1, without incorporating any disjunctive constraints. This means that the reference case includes only the basic MILP–based constraints for BESs, without considering the advanced technical constraints, detailed pricing models, or subsidy policies. This makes it an ideal baseline to illustrate the impact of integrating different disjunctive constraints.

The benchmark scenario is based on a multifamily house located in Düsseldorf, Germany. The house has a living area of 500 square meters and is equipped with 50 m^2 designated for photovoltaic and solar thermal panels. The energy requirements of the building include hot water, space heating, and electricity, with annual demand curves shown in Figure 3.

The superstructure of the equipment connections is illustrated in Figure 4, focusing on the operational limitations of the heat pump in meeting high temperature hot water demands. This superstructure includes two different storage units: the hot water storage and the heat storage. The hot water storage, designed for temperatures above 60°C, is exclusively charged by either the gas boiler or the electrical boiler. In contrast, the heat storage, which operates at a lower temperature threshold of 40°C, can be charged by the gas boiler, the heat pump, and the solar thermal panel. This heat storage is dedicated to the sole purpose of supplying energy to the underfloor heating system.

Beyond the reference case, six different use cases with the same connection configuration are explored, each integrating different GDP models to address specific design and operational challenges. These cases are designed to demonstrate the versatility and increased accuracy of GDP in modeling complex devices and economic considerations in BESs. The specific attributes and modifications applied in each case are summarized in Table 3, which outlines the differences from the reference case.

In the reference case, all equipment prices are modeled using a unit cost approach with no fixed base cost. In contrast, the base price case and discrete price case use the GDP framework to model the gas boiler, heat pump, solar thermal panel, hot water storage, and heat storage, as detailed in Section 2.2.2. More detailed pricing information for these devices is provided in Figure A1, based on publicly available data through 2022. In the absence of specific market price information, photovoltaic panels and batteries continue to use the unit cost approach without a fixed base price.

For the subsidy cases (subsidy, subsidy + base price, subsidy + discrete price), multiple subsidies derived from different policies are considered. These include the German Federal Government's incentives for the use of renewable energy (EEG) [34], the Federal

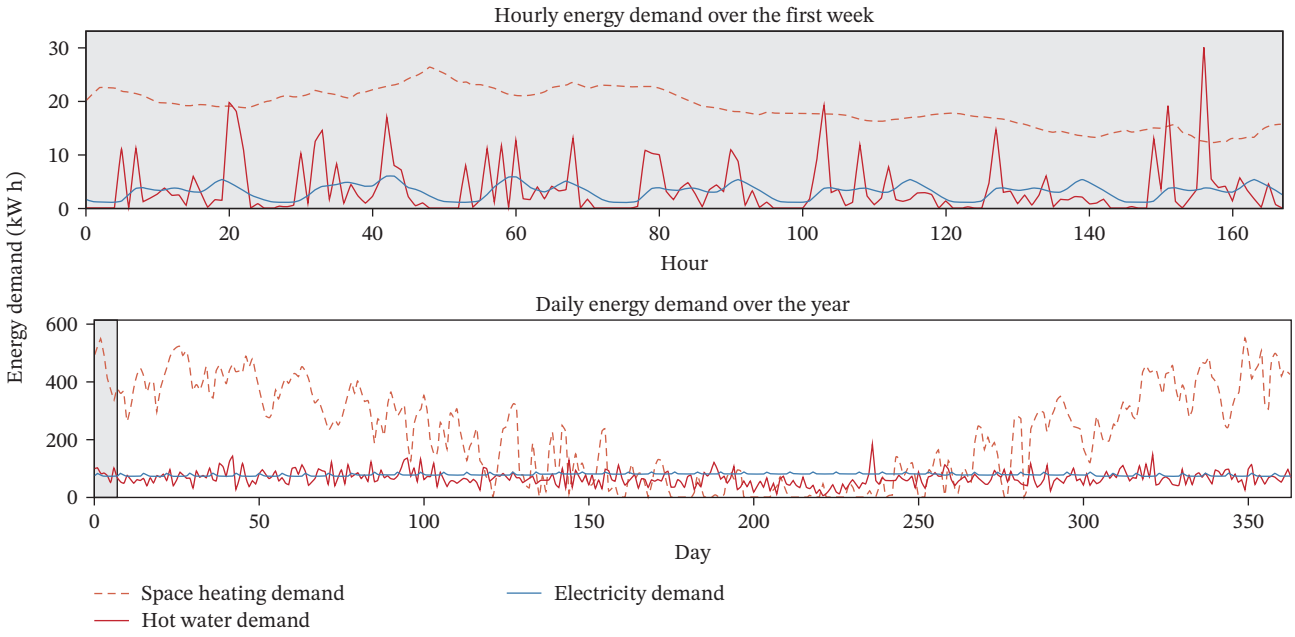

FIGURE 3 | Annual demand curves for hot water, space heating, and electricity.

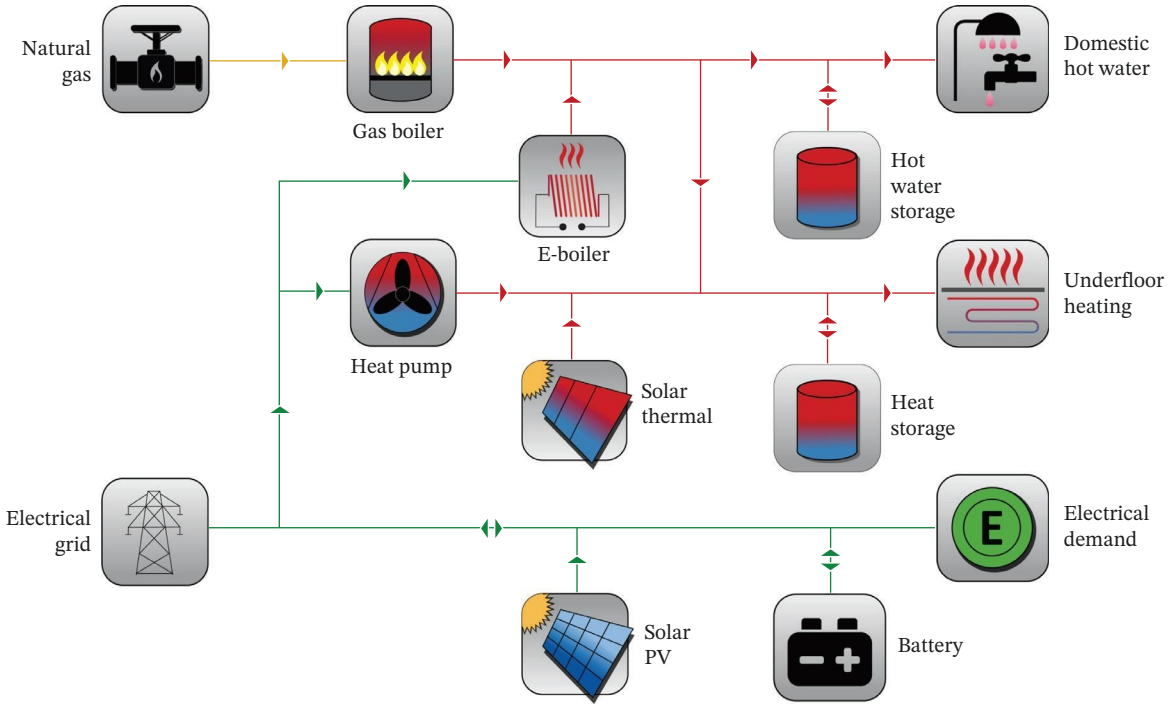

FIGURE 4 | Possible equipment connection configuration in the building.

Government's subsidies for the reduction of energy consumption in buildings (BEG EM) [35], and the local government of Düsseldorf's initiatives to promote the renovation of environmentally friendly buildings [36]. The model selectively applies subsidies based on the building type, with specific rules used in the model documented in Appendix A.

EEG subsidies are structured to incentivize the production of renewable energy based on the output capacity of installed systems. These subsidies provide a financial reward for the electricity produced, which can either be consumed on site or exported to the grid. Specifically, the EEG provides different subsidy modes tailored to specific operational strategies: one mode prioritizes meeting the immediate electricity demands of the building, while another model is optimized to maximize the export of electricity to the grid. These modes are designed to be mutually exclusive to ensure that each facility operates under the most appropriate economic conditions. The BEG EM program, along with local Düsseldorf subsidies, specifically supports the purchase of energy-efficient equipment. By providing financial incentives for the purchase of such technologies, these programs help lower the initial investment barriers and encourage broader adoption of energy-saving solutions.

TABLE 3 | Summary of use cases incorporating different GDP models.

Case	Description
Reference	Only MILP for optimization
Part load	GDP model with part load constraints for gas boilers and heat pumps
Base price	Fixed base price model for gas boilers, heat pumps, electric boilers, and storage
Discrete price	Discrete price model from actual market-based device options
Subsidy	Both purchase and operational subsidies applied within the reference case
Subsidy + base price	Both purchase and operational subsidies applied within the base price case
Subsidy + discrete price	Both purchase and operational subsidies applied within the discrete price case

4 | Results

Section 4 presents the results of applying the integrated GDP framework, which includes both MILP and GDP components, to optimize BESs. The analysis is divided into four parts: device selection, operational analysis, economic analysis, and computational cost comparison. Each part contributes to a comprehensive understanding of system performance under different scenarios.

4.1 | Device Selection

The analysis of device selection across different case scenarios, as shown in Figure 5, reveals the profound impact of economic models and subsidy frameworks on energy system configurations. Photovoltaic panels and gas boilers are consistently selected across all scenarios, indicating their fundamental role in meeting the building's energy needs. In each scenario, the size of the photovoltaic systems is uniformly set at 9 kWp, due to limitations on the maximum area of installable solar devices. Despite the availability of subsidies for solar thermal panels, their selection remains limited compared to photovoltaic panels, which offer superior electricity output and easier integration into the grid, providing greater utility and return on investment.

However, the selection of heat pumps and boilers shows significant variability, influenced by economic conditions and the presence of subsidies. In scenarios without subsidies, such as the base price and discrete price cases, heat pumps are often omitted due to prohibitive costs and lack of suitable models in these price categories. Conversely, the reference case features a small 2.18 kW heat pump that, despite its minimal capacity, demonstrates significant economic efficiency by operating at full load for 307 h per year. The economic analysis underscores a critical finding: larger gas boilers are favored in the discrete price model without subsidies due to their cost-effectiveness at higher capacities.

The introduction of part load constraints further complicates device selection, necessitating smaller devices that, while less economically efficient due to their limited operating hours, illustrate the delicate balance between system capacity and economic viability. The scenarios that include subsidies show a marked preference for larger and more efficient heat pumps, highlighting the role of financial incentives in encouraging the adoption of more capable systems.

4.2 | Operational Analysis

Pricing models and subsidy policies have a significant impact on device selection, which in turn affects operational performance. Although part load constraints have minimal impact on operational profiles during the high demand winter months, their impact is more pronounced during the lower demand transitional seasons. This divergence in operational impact under different demand conditions is illustrated in the following operational analysis. Figures 6 and 7 illustrate how the part load case more

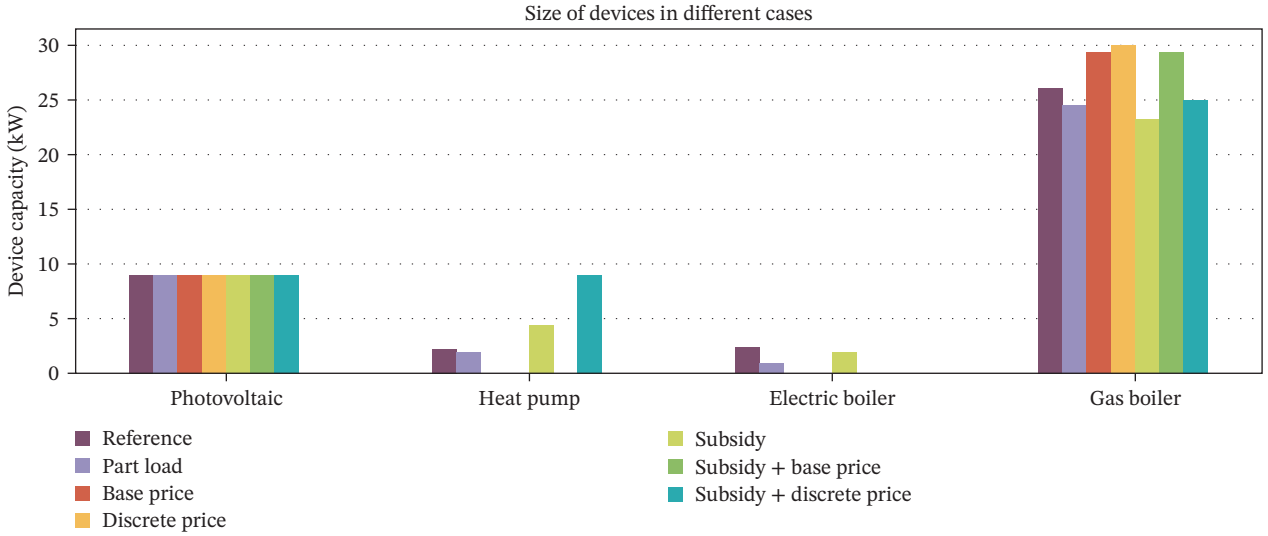

FIGURE 5 | Comparison of device selection across different cases, highlighting variations in equipment choice based on economic and subsidy conditions.

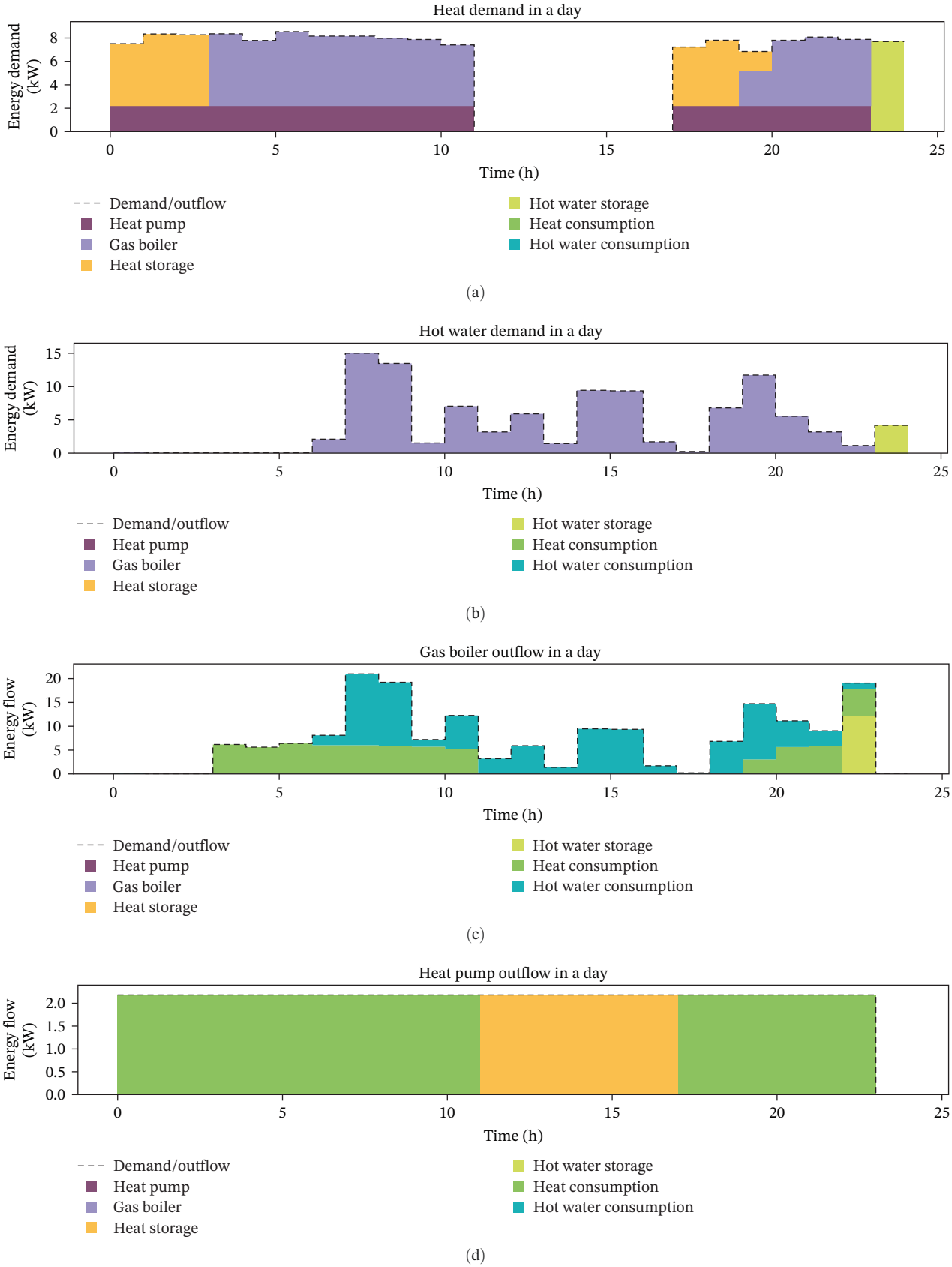

FIGURE 6 | Energy supply and flow for heating and hot water on a low-demand day in the Reference Case (without part-load constraints). (a) Composition of heat supply to meet space heating demand (dashed line). (b) Composition of heat supply to meet domestic hot water demand (dashed line). (c) Destination of the gas boiler's output energy. (d) Destination of the heat pump's output energy. In Subparts (c, d), the dashed line represents the device's total output and stacked colors show how that output is allocated.

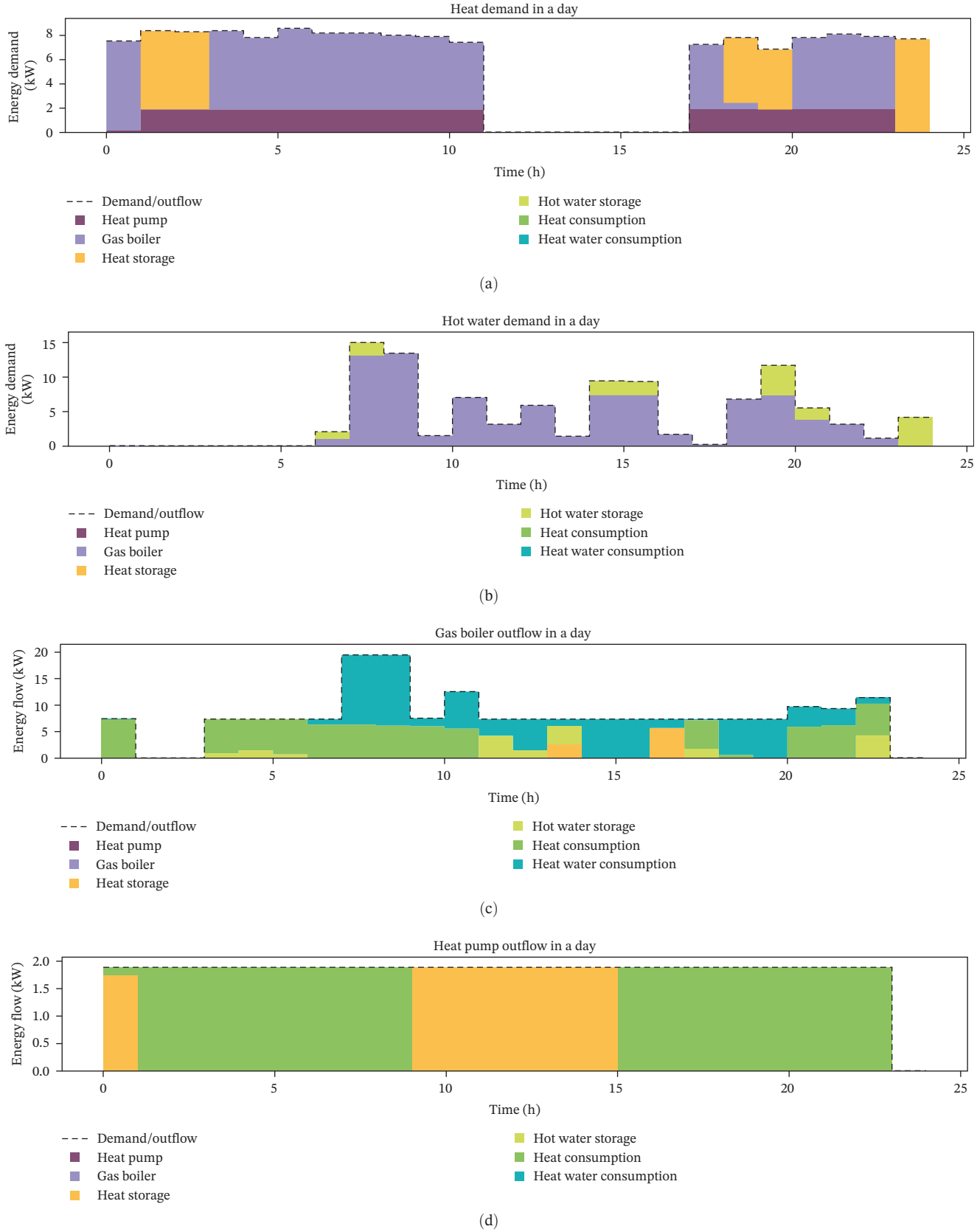

FIGURE 7 | Energy supply and flow for heating and hot water on the same low-demand day in the Part Load Case (with part-load constraints). (a) Composition of heat supply to meet space heating demand (dashed line). (b) Composition of heat supply to meet domestic hot water demand (dashed line). (c) Destination of the gas boiler's output energy. (d) Destination of the heat pump's output energy.

accurately reflects real-world operations by reducing the variability in equipment operation. This is achieved by including part load constraints that require the use of storage systems to absorb excess energy during low demand periods and release it when needed. In contrast, the reference case lacks this capability, resulting in greater operational variability.

The diagrams sequentially show the sources that meet the heating and hot water demand, followed by the energy flow dynamics of gas boilers and heat pumps that are subject to part load constraints. Comparative analysis of these diagrams shows that both scenarios similarly rely on heat pumps for the base energy supply, while gas boilers provide the primary energy supply.

In the early hours, discrepancies in energy supply are observed, largely due to variations in stored energy from the previous day's hot water storage. By the third hour, the energy stored in the heat storage tanks is completely exhausted in both cases, after which the systems rely mainly on the direct outputs of the heat pumps and gas boilers. Between 12:00 and 17:00, the heat pumps are mainly used to charge the heat storage tanks.

A significant difference occurs around midday, when part load constraints prevent the gas boiler from operating at the very low outputs typically required by fluctuating demand. Instead, any excess energy produced during these fluctuations is stored, resulting in a much more stable output compared to the reference case where no part load constraints are applied.

In addition, the analysis underscores the enhanced role of storage under part load constraints. Storage units for both high-temperature domestic hot water and low-temperature space heating show increased usage times—183 and 212 h, respectively, compared to 154 and 204 h in the reference case. This highlights the importance of storage systems in managing the operational flexibility and efficiency of the system under constrained conditions.

4.3 | Economic Analysis

Table 4 shows the economic impact of implementing various models, summarizing costs, subsidies, and revenues-including EEG subsidies. The discrete price case, which reflects real-world scenarios, where equipment options are limited to discrete sets, shows financial outcomes that closely approximate actual applications. In the absence of subsidies, the financial outcomes of the various pricing models show slight differences. Specifically, the total cost difference between the reference case and the discrete price case is marginal at −0.5%, while the base price case shows a more pronounced cost increase of +0.73%.

The introduction of subsidies reduces total annual costs by about 3%, significantly increasing the attractiveness of adopting more efficient technologies. Notably, even with purchase subsidies, the subsidy + discrete price case shows an increase in capital expenditures, while operating expenditures are significantly reduced due to the efficiency gains from using high efficiency heat pumps powered by photovoltaic electricity.

Furthermore, the economic comparisons between the scenarios show nuanced impacts under subsidy conditions: the difference between the reference case with linear pricing and the discrete price case is −0.2%, while the base price case shows a more significant difference of 1.6%.

Moreover, the optimized selection of EEG modes in these subsidized scenarios consistently favors surplus electricity supply to the grid compared to full feed-in mode. This strategic choice makes better use of limited rooftop space more effectively by prioritizing internal electricity demand and thermal energy production through heat pumps over exporting electricity. The economic advantages of this strategy are reflected in the relatively lower revenues from electricity export, which are more than offset for by the savings and EEG subsidies attributed to on-site consumption and surplus electricity export.

4.4 | Computational Cost Analysis for Big-M and Convex Hull

In addition to analyzing the impact of GDP on BESs, a computational cost comparison was performed between the big-M and convex hull methods across different use cases to evaluate the impact of GDP on model optimization performance. Use cases involving subsidies were excluded from this comparison because certain subsidy policies introduce nonlinearities into the model that make the convex hull method inapplicable. To evaluate performance over different problem scales, the comparison was conducted by varying the number of typical days (10, 16, and 30) and by considering a full year optimization without temporal clustering (365 days).

The results, as shown in the Figure 8, highlight the computation times for the reference case, part load case, base price case, and discrete price case. In the reference case, since no GDP–related variables were involved, the computation times for the big-M and

TABLE 4 | Comparison of economic parameters across different cases.

Cases	Total cost (Euro)	OPEX (Euro)	CAPEX (Euro)[a]	Revenue (Euro)	Purchase subsidy (Euro)
Reference	16,997	15,166	1834	3	0
Part load	17,067	15,331	1783	47	0
Base price	17,205	15,561	1752	108	0
Discrete price	17,081	15,588	1601	108	0
Subsidy	16,563	14,942	2096	3	471
Subsidy + base price	16,857	15,561	1752	116	339
Subsidy + discrete price	16,590	14,651	2530	21	570

[a]CAPEX values do not include purchase subsidies.

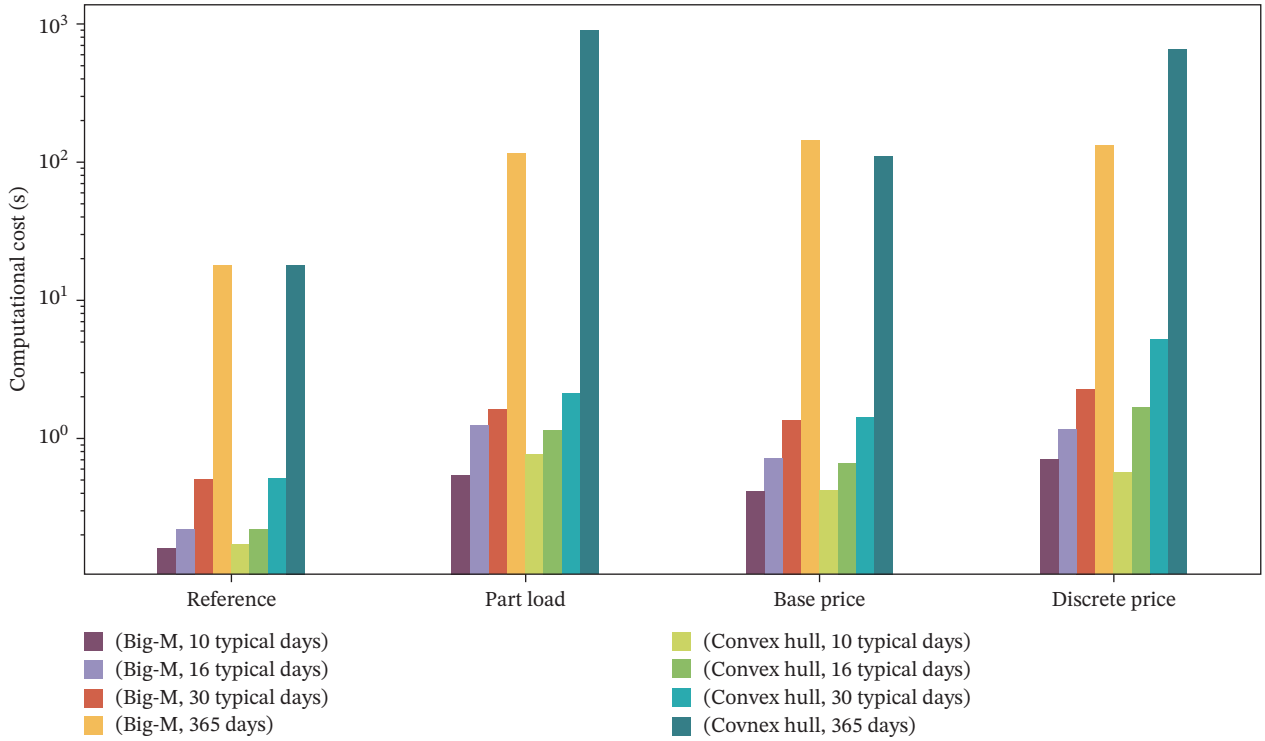

FIGURE 8 | Computational time comparison of Big-M and convex hull methods across the reference, part load, base price, and discrete price cases. Subsidy scenarios are excluded from this comparison because the associated nonlinear formulations cannot be handled by the convex hull method.

convex hull methods were identical. In simpler use cases with fewer disjunctive constraints, such as the base price case, there was little difference in computation times between the two methods for typical day scenarios. In the full year simulation (365 days), the convex hull method performed slightly better, with a computation time of 110 s compared to 144 s for the big-M method, representing a 23.6% reduction.

However, in more complex scenarios, such as the discrete price case and part load case, the performance gap between the methods became more pronounced as the number of days increased. For optimizations with 10 and 16 typical days, the running times for the convex hull and big-M methods remained comparable. As the model size increased, especially in the 365-day optimization, the convex hull method's computation time significantly exceeded that of the big-M method. In the discrete price case and part load case, the convex hull method took 4 and 6.7 times longer than the big-M method, respectively.

In addition to runtime, solver performance also depends strongly on formulation structure and the tightness of the continuous relaxation. Table 5 summarizes these metrics for representative 10- and 30-day cases. Convex hull formulations consistently introduce additional variables and constraints compared to big-M, reflecting their more detailed representation of disjunctions. This structural difference results in substantially tighter continuous relaxations in the discrete price and fixed price cases (reducing the relaxation gap from around 5% with big-M to below 1%–2% with convex hull). In contrast, for part-load cases, both methods already yield very tight relaxations (gaps below 0.1%). These results demonstrate that the choice between big-M and convex hull not only affects runtime performance but also the underlying mathematical properties of the formulation.

5 | Discussions

In the case studies, a notable discrepancy was observed between the subsidy + discrete price case and the subsidy + base price case, wherein the former selected a heat pump while the latter did not. This outcome can be attributed to the inclusion of specific device options in the subsidy plus discrete price case that, despite their larger size, are available at lower prices. These options offer superior cost effectiveness in comparison to the fitted price curves utilized in the subsidy + discrete price case. In practical scenarios, such price discrepancies may result from variations between brands or different models of devices.

Nevertheless, the selection of more economical devices may entail other compromises, such as reduced efficiency or elevated maintenance expenses over the device's lifespan. The current model does not account for these factors; thus, addressing this issue would necessitate the specification of the efficiency and long-term operational costs for each equipment option. The incorporation of efficiency as a variable would result in the introduction of nonlinearity into the model, thereby affecting the overall optimization process.

Notably, the part-load constraints, while substantially altering operational schedules, led to only a modest increase in total annualized cost (0.4% in the part load case vs. the reference case in Table 4). This indicates that the system adapted to the technical constraint primarily through operational flexibility-increased utilization of thermal storage-rather than through costly over-sizing of equipment. This finding demonstrates how the GDP–augmented model can identify cost-effective operational adaptations to meet technical requirements, which might be overlooked in simpler formulations.

TABLE 5 | Structural metrics and continuous relaxation gaps for representative cases.

Case	Method	#Vars (binary)	#Constr	Cont. relax gap (%)
Reference (10 days)	—	14,303 (0)	13,498	0.0
Part load (10 days)	Big-M	15,359 (1056)	15,610	0.04
	Conv hull	17,471 (1056)	17,722	0.04
Fixed price (10 days)	Big-M	14,313 (10)	13,533	4.8
	Conv hull	14,333 (10)	13,538	1.6
Discrete price(10 days)	Big-M	14,469 (166)	14,162	5.3
	Conv hull	14,801 (166)	14,162	0.7
Reference (30 days)	—	40,223 (0)	37,978	0.0
Part load (30 days)	Big-M	43,199 (2976)	43,930	0.05
	Conv hull	49,151 (2976)	49,882	0.05
Fixed price (30 days)	Big-M	40,233 (10)	38,013	4.8
	Conv hull	40,253 (10)	38,018	1.7
Discrete price(30 days)	Big-M	40,389 (166)	38,642	5.3
	Conv hull	40,721 (166)	38,642	0.8

As is the case with the majority of BES optimization models that employ MILP, the GDP model employs a 1-h time step. However, with regard to operational performance, this time interval may prove to be excessive for residential energy systems, which are typically more flexible. Smaller systems may cycle on and off within an hour, which in reality reduces the effective part-load ratio compared to the 1-h model representation. Consequently, the model enforces a minimum device runtime of 1 h, which can be substantially longer than the actual minimum cycling time of certain residential equipment (e.g., heat pumps or boilers that can modulate within minutes). This behavior is not explicitly modeled through ramping constraints, but rather approximated via the chosen time resolution. The use of a smaller time step interval in the model may enhance its capacity to capture short-term fluctuations, thereby facilitating a more precise representation of operational behavior. Nevertheless, this approach would inevitably result in a greater computational burden and necessitate more comprehensive input data, which may not always be readily accessible.

The results demonstrate that subsidy policies exert a considerable influence on equipment selection and the overall economic viability of a system, particularly in instances where subsidies render otherwise costly equipment, such as heat pumps, more economically feasible. While the pricing model itself had a negligible effect on total costs, the presence of subsidies was of critical importance in influencing long-term operational expenditures and upfront capital investments. These economic outcomes are contingent upon external boundary conditions, such as energy prices and the possibility of combining multiple subsidies. Given the significant variation in these factors across regions, it is imperative to conduct localized economic analyses to ensure the optimization process is tailored to specific conditions. The GDP framework developed in this study is inherently adaptable to different subsidy structures. The tiered subsidy model presented in Section 2.2.3 serves as a template that can be easily parameterized or extended to represent the logic of policies from other countries or regions. Future applications would primarily require updating the disjunctive rules and the corresponding subsidy amounts according to local regulations, without altering the core optimization framework.

The computational comparison reveals a fundamental trade-off between model compactness and relaxation tightness. The big-M method yields smaller MILP models (fewer variables and constraints), while the convex hull method provides a tighter continuous relaxation at the expense of a larger problem size. For smaller problems (e.g., optimizations with 10 or 16 typical days), this trade-off is often balanced, and the convex hull method can sometimes offer slight advantages due to its tighter relaxation. However, as model complexity increases-especially in full-year optimizations or in cases with numerous time-coupled binary variables like the part load and discrete price scenarios—the model size penalty of the convex hull reformulation becomes dominant, leading to significantly longer solve times (e.g., 4–6.7 times slower) compared to the more compact big-M formulation. This indicates that the benefit of a tighter relaxation is contingent on the nature of the disjunctions. For problems dominated by many time-step-dependent decisions, the compactness of big-M is the decisive factor. For problems with few strategic and non-temporal disjunctions (e.g., discrete device selection in smaller models), the convex hull's tighter relaxation may justify its use. Consequently, a practical guideline for practitioners is to prefer big-M for large-scale models or those with extensive temporal disjunctions, and to consider convex hull for smaller-scale problems where its relaxation advantage might be leveraged.

These findings align with previous studies, which have shown that convex hull formulations provide tighter relaxations, but typically introduce additional variables and constraints, leading to increased computational burden as model size grows. To improve scalability, several directions appear promising. First, decomposition techniques (e.g., Benders or Dantzig–Wolfe decomposition) could partition the large-scale MILP into more tractable

subproblems. Second, warm-start strategies that use solutions from big-M formulations or heuristic methods as initial points may help reduce solution times for convex hull models. Third, hybrid reformulations that selectively apply convex hull to critical disjunctions while retaining big-M elsewhere could balance relaxation tightness and computational efficiency. Exploring such strategies in future studies may substantially enhance the applicability of convex hull reformulations to large-scale BES optimization. Furthermore, hybrid reformulation strategies, which selectively apply the convex hull method to critical disjunctions while using the big-M method for others, present a promising direction to balance solution tightness and computational efficiency. While a detailed investigation of such hybrid strategies is beyond the scope of this study, future work could systematically evaluate their performance across a range of BES optimization problems to provide practitioners with clearer selection guidelines.

6 | Conclusions and Outlook

This paper examines the enhancement of BES design optimization through the incorporation of disjunctive formulations within the GDP framework, showcasing their implementation in three pivotal areas: part load constraints, discrete price models, and subsidy models. The study employs a comprehensive use case with multiple model scenarios to illustrate the substantial impact of these integrated disjunctive constraints on system performance and decision-making.

The findings indicate that part load constraints have a more pronounced effect on short-term operational strategies than on the total annualized cost or final equipment selection in the studied cases. Their impact on device scheduling and storage utilization is significant, particularly during periods of low demand, as detailed in Section 5. The impact of price models on equipment selection is significant, primarily due to the limitations of the MILP model, which assumes the availability of nonexistent market devices. The base price case produces results that are more closely aligned with those of an accurate discrete model, underscoring the significance of realistic pricing strategies in system optimization. The results demonstrate that subsidies exert a considerable influence on both device selection and economic analysis, serving as a pivotal instrument for incentivizing the adoption of efficient technologies in the scenarios.

The diverse applications of the GDP model illustrate its capacity to augment the conventional MILP model by addressing particular operational or economic concerns. The GDP model offers a more flexible and adaptive tool for designing BESs, regardless of whether the concern is operational dynamics, as addressed through part load constraints, or device selection and financial considerations, as influenced by pricing models and subsidies.

The application of the GDP model entails substantial computational costs, largely due to the necessity of handling disjunctive constraints, as seen in operational dynamics models and subsidy calculations. To address these challenges, two common reformulation methods are employed: the big-M method and the conevex hull method. Although both methods are capable of effectively transforming GDP models into MILP formulations, they exhibit distinct differences in computational efficiency. To illustrate, in smaller models comprising fewer typical days, the convex hull method offers a slight computational advantage, despite introducing additional variables and constraints, its tighter relaxation can sometimes reduce branch-and-bound effort. Nevertheless, in full-year simulations (365 days), the convex hull method markedly reduces the computational time in comparison to the big-M method. In the part load case, the convex hull method required 893.21 s, whereas the big-M method required only 115.15 s, representing a nearly six-and-a-half-fold increase. Similarly, in the discrete price case, the convex hull method required four times the computational time of the big-M method.

Further research could concentrate on incorporating the GDP model into the design phase of building energy control systems, in order to anticipate and address the potential for significantly increased computational demands. It would be beneficial to investigate the potential of efficient solving strategies for large-scale models with numerous binary variables in the GDP model. One avenue for exploration could be the use of MILP model solutions as initial points. Future work could also investigate the sensitivity of optimal designs to fluctuations in equipment market prices, integrating stochastic or robust optimization techniques with the GDP framework presented here. Furthermore, extending the application of the GDP model to district-level energy systems could present new avenues for enhancing energy optimization on a larger scale.

Nomenclature

Abbreviations

GDP:	Generalized disjunctive programming
MILP:	Mixed-integer linear programming

Greek Symbols

α:	Minimum part-load ratio
δ:	Connection status indicator
η:	Efficiency (in/out, self-discharge)
τ:	Length of one typical day (24 h)

Indices and Sets

$d \in D$:	Device index
$e \in E$:	Energy carrier (e.g., electricity and heat)
$i \in \{1,\ldots,N\}$:	Index of typical days
$k \in K$:	Device option index
N:	Number of typical days
$t \in T$:	Time step (hourly index)
t_{last}:	Final time step of the full simulation horizon

Underscores

buy:	Device is purchased
feed:	Electricity feed-in
in:	Inflow/input
inv:	Investment

min:	Minimum part load
not:	Device is not purchased
on/off:	Device operational state (binary)
op:	Operation
out:	Outflow/output
rated:	Rated value
small, medium, large:	Discrete device size categories
tot:	Total cost

Variables

a:	Annualization factor
C:	Cost
E:	Energy
F:	Fixed cost component
P:	Power or capacity
R:	Revenue
S:	Subsidy
w:	Weight of a typical day in clustering
Y:	Boolean decision variable (disjunction).

Acknowledgments

The author would like to thank colleagues at the Institute for Energy Efficient Buildings and Indoor Climate (EBC), RWTH Aachen University, for their valuable support and discussions during this research.

Funding

This work was supported by the funding initiative of "FEN Research Campus–Public–Private Partnership for Innovation" from the Federal Ministry of Education and Research (BMBF), project "InEEd-DC" (Grant 03SF0597). Open Access funding enabled and organized by Projekt DEAL.

Conflicts of Interest

The authors declare no conflicts of interest.

Data Availability Statement

The datasets and model code used in this study are openly available at the GitHub repository: https://github.com/RWTH-EBC/BESDOT.

References

1. EU Energy in Figures: Statistical Pocketbook 2023, "Publications Office of the European Union," ISBN. 978-92-68-01165-2. OCLC: 1420514055 (2023).

2. H. F. Castleton, V. Stovin, S. B. M. Beck, and J. B. Davison, "Green Roofs; Building Energy Savings and the Potential for Retrofit," *Energy and Buildings* 42, no. 10 (2010): 1582–1591.

3. K. A. Barber and M. Krarti, "A Review of Optimization Based Tools for Design and Control of Building Energy Systems," *Renewable and Sustainable Energy Reviews* 160 (2022): 112359.

4. H. Sha, P. Xu, Z. Yang, Y. Chen, and J. Tang, "Overview of Computational Intelligence for Building Energy System Design," *Renewable and Sustainable Energy Reviews* 108 (2019): 76–90.

5. M. Wirtz, M. Hahn, T. Schreiber, and D. Müller, "Design Optimization of Multi-Energy Systems Using Mixed-Integer Linear Programming: Which Model Complexity and Level of Detail Is Sufficient?" *Energy Conversion and Management* 240 (2021): 114249.

6. R. Raman and I. E. Grossmann, "Modelling and Computational Techniques for Logic Based Integer Programming," *Computers & Chemical Engineering* 18, no. 7 (1994): 563–578.

7. I. E. Grossmann and J. P. Ruiz, "Generalized Disjunctive Programming: A Framework for Formulation and Alternative Algorithms for MINLP Optimization," in *Mixed Integer Nonlinear Programming*, eds. J. Lee and S. Leyffer, 154, (Springer, 2012): 93-93–115-115.

8. K. B. Lindberg, D. Fischer, G. Doorman, M. Korpås, and I. Sartori, "Cost-Optimal Energy System Design in Zero Energy Buildings With Resulting Grid Impact: A Case Study of a German Multi-Family House," *Energy and Buildings* 127 (2016): 830–845.

9. M. A. Lozano, J. C. Ramos, M. Carvalho, and L. M. Serra, "Structure Optimization of Energy Supply Systems in Tertiary Sector Buildings," *Energy and Buildings* 41, no. 10 (2009): 1063–1075.

10. E. Iturriaga, Á. Campos-Celador, J. Terés-Zubiaga, U. Aldasoro, and M. Álvarez-Sanz, "A MILP Optimization Method for Energy Renovation of Residential Urban Areas: Towards Zero Energy Districts," *Sustainable Cities and Society* 68 (2021): 102787.

11. C. Wouters, E. S. Fraga, and A. M. James, "An Energy Integrated, Multi-Microgrid, MILP (Mixed-Integer Linear Programming) Approach for Residential Distributed Energy System Planning—A South Australian Case-Study," *Energy* 85 (2015): 30–44.

12. D. C. Alvarado, S. Acha, N. Shah, and C. N. Markides, "A Technology Selection and Operation (TSO) Optimisation Model for Distributed Energy Systems: Mathematical Formulation and Case Study," *Applied Energy* 180 (2016): 491–503.

13. Y. Kuang, M. Hu, R. Dai, and D. Yang, "A Collaborative Decision Model for Electric Vehicle to Building Integration," *Energy Procedia* 105 (2017): 2077–2082.

14. T. Schütz, L. Schiffer, H. Harb, M. Fuchs, and D. Müller, "Optimal Design of Energy Conversion Units and Envelopes for Residential Building Retrofits Using a Comprehensive MILP Model," *Applied Energy* 185 (2017): 1–15.

15. E. Iturriaga, U. Aldasoro, J. Terés-Zubiaga, and A. Campos-Celador, "Optimal Renovation of Buildings Towards the Nearly Zero Energy Building Standard," *Energy* 160 (2018): 1101–1114.

16. D. Steen, M. Stadler, G. Cardoso, M. Groissböck, N. DeForest, and C. Marnay, "Modeling of Thermal Storage Systems in MILP Distributed Energy Resource Models," *Applied Energy* 137 (2015): 782–792.

17. F. Rossi, M. Heleno, R. Basosi, and A. Sinicropi, "Environmental and Economic Optima of Solar Home Systems Design: A Combined LCA and LCC Approach," *Science of the Total Environment* 744 (2020): 140569.

18. J. R. Jackson and I. E. Grossmann, "A Disjunctive Programming Approach for the Optimal Design of Reactive Distillation Columns," *Computers & Chemical Engineering* 25, no. 11-12 (2001): 1661–1673.

19. H. Yeomans and I. E. Grossmann, "A Systematic Modeling Framework of Superstructure Optimization in Process Synthesis," *Computers & Chemical Engineering* 23, no. 6 (1999): 709–731.

20. V. C. Onishi, N. Quirante, M. A. S. S. Ravagnani, and J. A. Caballero, "Optimal Synthesis of Work and Heat Exchangers Networks Considering Unclassified Process Streams at Sub and Above-Ambient Conditions," *Applied Energy* 224 (2018): 567–581.

21. V. C. Onishi, M. A. S. S. Ravagnani, and J. A. Caballero, "Retrofit of Heat Exchanger Networks With Pressure Recovery of Process Streams at Sub-Ambient Conditions," *Energy Conversion and Management* 94 (2015): 377–393.

22. A. Bhattacharya, X. Ma, and D. L. Vrabie, "Model Predictive Control of Discrete-Continuous Energy Systems via Generalized Disjunctive Programming," *IFAC-PapersOnLine* 54, no. 20 (2021): 913–918.

23. D. Kim, T. Hong, and M. A. Piette, "Generalized Disjunctive Programming-Based, Mixed Integer Linear MPC Formulation for Optimal Operation of a District Energy System for PV Self-Consumption and Grid Decarbonization: Field Implementation," (2022).

24. S. Cho, J. Tovar-Facio, and I. E. Grossmann, "Disjunctive Optimization Model and Algorithm for Long-Term Capacity Expansion Planning of Reliable Power Generation Systems," *Computers & Chemical Engineering* 174 (2023): 108243.

25. N. Stewart, B. Arguello, M. Hoffman, B. Nicholson, and R. Garrett, "Optimal Mitigation and Control Over Power System Dynamics for Stochastic Grid Resilience," *Optimization and Engineering* 25, no. 2 (2024): 911–940.

26. J. I. Manassaldi, N. J. Scenna, and S. F. Mussati, "Optimization Mathematical Model for the Detailed Design of Air Cooled Heat Exchangers," *Energy* 64 (2014): 734–746.

27. M. L. Bynum, G. A. Hackebeil, W. E. Hart, et al., "Pyomo-Optimization Modeling in Python," in *Springer Optimization and Its Applications*, 67, (Springer International Publishing, 2021).

28. Gurobi Optimization, LLC, "Gurobi Optimizer Reference Manual," 2023, https://www.gurobi.com/documentation/.

29. D. Y. Lee, B. M. Seo, Y. B. Yoon, S. H. Hong, J. M. Choi, and K. H. Lee, "Heating Energy Performance and Part Load Ratio Characteristics of Boiler Staging in an Office Building," *Frontiers in Energy* 13, no. 2 (2019): 339–353.

30. Q. Chen, E. S. Johnson, D. E. Bernal, et al., "Pyomo.GDB: An Ecosystem for Logic-Based Modeling and Optimization Development," *Optimization and Engineering* 23, no. 1 (2022): 607–642.

31. H. Paul Williams, *Model Building in Mathematical Programming* (John Wiley & Sons, 2013).

32. S. Lee and I. E. Grossmann, "New Algorithms for Nonlinear Generalized Disjunctive Programming," *Computers & Chemical Engineering* 24, no. 9-10 (2000): 2125–2141.

33. N. W. Sawaya and I. E. Grossmann, "A Cutting Plane Method for Solving Linear Generalized Disjunctive Programming Problems," *Computers & Chemical Engineering* 29, no. 9 (2005): 1891–1913.

34. German Federal Government, "Erneuerbare-energien-gesetz," 2023, https://www.gesetze-im-internet.de/eeg_2014/.

35. German Federal Ministry for Economic Affairs and Energy, "Bundesförderung für energieeffizienz in der gebäudehülle," 2023, https://www.bafa.de/DE/Energie/Effiziente_Gebaeude/Sanierung_Wohngebaeude/Anlagen_zur_Waermeerzeugung/anlagen_zur_waermeerzeugung_node.html.

36. City of Düsseldorf, "Förderprogramm Klimafreundliches Wohnen und Arbeiten in düsseldorf: Richtliniennovelle 2023," 2023, https://www.duesseldorf.de/umweltamt/projekte/klimafreundliches-wohnen-und-arbeiten.

Appendix

Appendix A. Supplementary Data

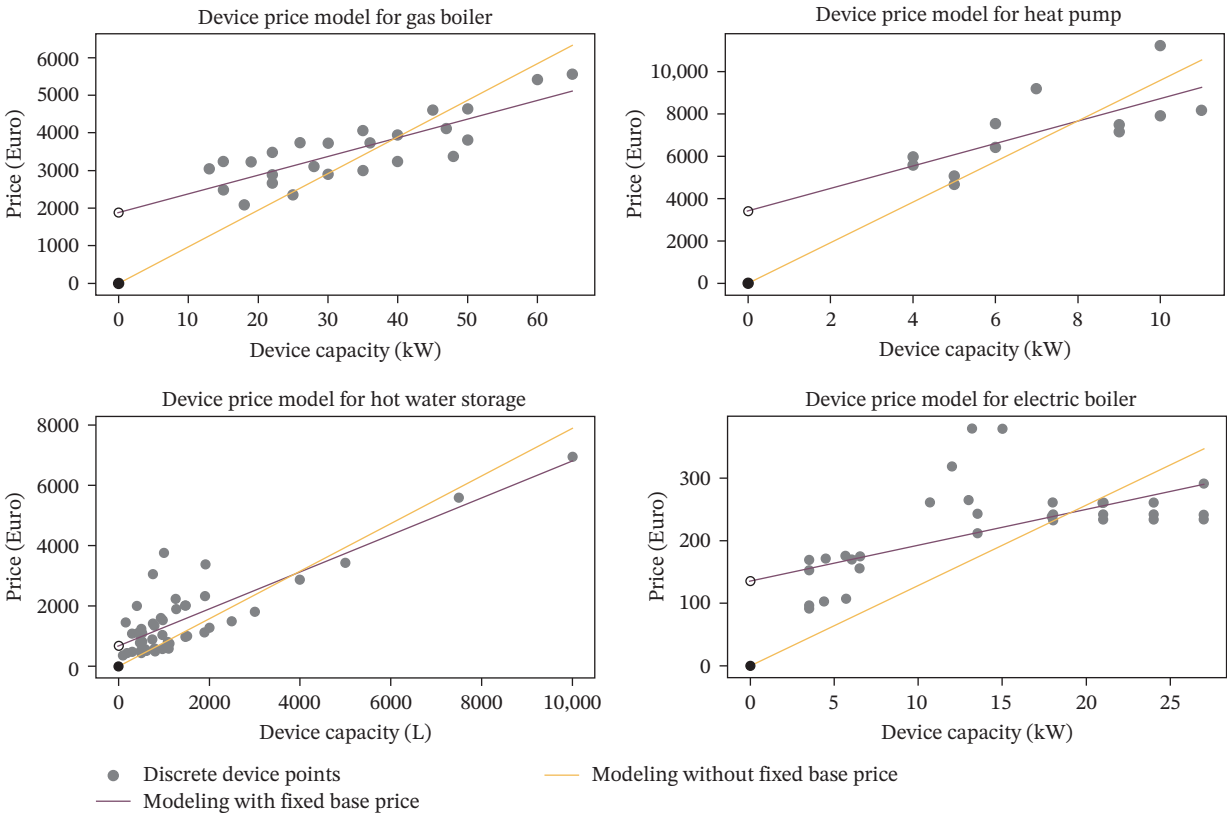

FIGURE A1 | Size of devices in use case.

TABLE A1 | Subsidy rules for new buildings in Düsseldorf, categorized by device type and capacity range.

Device	Capacity range	Total subsidy amount
Photovoltaic	0.6 to 10 kWp	300 Euro per kWp
	10 to 45 kWp	3000 Euro + 200 Euro per kWp above 10 kWp
	≥ 45 kWp	10,000 Euro
Solar thermal panel	4–20 kWp	200 Euro per kWp
	≥ 20 kWp	120 Euro per kWp
Battery	≥ 0 kWh	250 Euro per kW h

TABLE A2 | Subsidy rules under the BEG EM program for new buildings, applicable to selected devices.

Device	Minimum investment required	Subsidy amount
Heat pump	≥ 2000 Euro	25% of investment
Solar thermal panel	≥ 2000 Euro	25% of investment

TABLE A3 | Subsidy rules under EEG for photovoltaic systems, detailing rates for various operation modes and capacity ranges.

Mode	Capacity range (kWp)	Subsidy amount (Euro/kW h)
Surplus feed-in	0–10	0.082
	10–40	0.071
	40–100	0.058
	≥ 100	0.0
Full feed-in	0–10	0.130
	10–100	0.109
	≥ 100	0.0

Appendix B. Methodological Details

Appendix B1. Big-M Reformulation

A general disjunction in GDP can be expressed as:

$$\bigvee_{j\in J}\begin{bmatrix} Y_j \\ r_j(x)\le 0\end{bmatrix},\ \sum_{j\in J} Y_j = 1,\ Y_j\in\{0,1\}.$$

In the big-M approach, each disjunctive constraint is relaxed by a sufficiently large constant M_j, yielding:

$$r_j(x)\ \le\ M_j\big(1-Y_j\big),\ \forall j\in J.$$

Example: Minimum Part-Load Constraint With On/Off States. Consider the disjunction describing whether a device is operating above its minimum part-load ratio α or completely off (cf. Equation (11)):

$$\begin{bmatrix} Y_{\text{on}} \\ P_{\text{out}}\ge \alpha\, P_{\text{rated}}\end{bmatrix}\ \veebar\ \begin{bmatrix} Y_{\text{off}} \\ P_{\text{out}}=0\end{bmatrix},\ Y_{\text{on}}+Y_{\text{off}}=1.$$

The big-M reformulation introduces explicit constraints for both the on and off branches:

$$\begin{aligned} P_{\text{out}}\ &\ge\ \alpha\, P_{\text{rated}} - M_{\text{on}}(1-Y_{\text{on}}),\\ P_{\text{out}}\ &\le\ M_{\text{off}}(1-Y_{\text{off}}),\\ P_{\text{out}}\ &\ge\ -M_{\text{off}}(1-Y_{\text{off}}),\\ Y_{\text{on}}+Y_{\text{off}}&=1,\ Y_{\text{on}},Y_{\text{off}}\in\{0,1\},\\ 0\le P_{\text{out}}&\le U_{\text{out}},\ 0\le P_{\text{rated}}\le U_{\text{rated}}. \end{aligned}$$

Here, $M_{\text{on}}\ge\alpha U_{\text{rated}}$ and $M_{\text{off}}\ge U_{\text{out}}$ are chosen from known bounds. The second and third constraints ensure that $P_{\text{out}}=0$ when $Y_{\text{off}}=1$. In most engineering applications, P_{out} is inherently nonnegative. Therefore, the lower bound $-M_{\text{off}}(1-Y_{\text{off}})$ is redundant and can be omitted in practice, since it is always satisfied when $P_{\text{out}}\ge 0$. This simplification reduces one redundant inequality without affecting model logic.

Appendix B2. Convex Hull Reformulation

In contrast to the big-M method, the convex hull reformulation represents the feasible region of each disjunctive constraint more tightly by introducing additional variables and constraints. A general disjunction can be expressed as:

$$\bigvee_{j\in J}\begin{bmatrix} Y_j \\ r_j(x)\le 0 \end{bmatrix},\ \sum_{j\in J} Y_j = 1,\ Y_j\in\{0,1\}.$$

In the convex hull approach, each term $r_j(x)\le 0$ is reformulated by scaling with the binary variable Y_j, and by introducing a copy of the continuous variables for each disjunct:

$$r_j(\widehat{x}_j)\ \le\ 0,\ \widehat{x}_j = x\cdot Y_j,\ \forall j\in J.$$

The linking condition:

$$x=\sum_{j\in J}\widehat{x}_j,$$

ensures that exactly one set of variables is active when $Y_j=1$. This results in a tighter polyhedral representation than big-M, but at the expense of a larger number of variables and constraints.

Example: Minimum Part-Load Constraint With On/Off States. Taking the same disjunction as in Equation (11), the convex hull reformulation introduces variable copies $(\widehat{P}_{\text{out,on}},\widehat{P}_{\text{rated,on}})$ and $(\widehat{P}_{\text{out,off}},\widehat{P}_{\text{rated,off}})$, linked by:

$$P_{\text{out}}=\widehat{P}_{\text{out,on}}+\widehat{P}_{\text{out,off}},\ P_{\text{rated}}=\widehat{P}_{\text{rated,on}}+\widehat{P}_{\text{rated,off}}.$$

The constraints are then:

$$\begin{aligned}
&\widehat{P}_{\text{out,on}}\ \ge\ \alpha\,\widehat{P}_{\text{rated,on}},\\
&\widehat{P}_{\text{out,off}}=0,\\
&0\le\widehat{P}_{\text{out,on}}\le U_{\text{out}}Y_{\text{on}},\ 0\le\widehat{P}_{\text{rated,on}}\le U_{\text{rated}}Y_{\text{on}},\\
&0\le\widehat{P}_{\text{out,off}}\le U_{\text{out}}Y_{\text{off}},\ 0\le\widehat{P}_{\text{rated,off}}\le U_{\text{rated}}Y_{\text{off}},\\
&Y_{\text{on}}+Y_{\text{off}}=1,\ Y_{\text{on}},Y_{\text{off}}\in\{0,1\}.
\end{aligned}$$

Note that in theory the convex hull reformulation introduces $\widehat{P}_{\text{out,on}}=P_{\text{out}}Y_{\text{on}}$ and $\widehat{P}_{\text{out,off}}=P_{\text{out}}Y_{\text{off}}$. Since these expressions are bilinear, practical MILP solvers use linear inequalities (bounds such as $0\le\widehat{P}_{\text{out,on}}\le U_{\text{out}}Y_{\text{on}}$) to represent them. Together with the linking constraint $P_{\text{out}}=\widehat{P}_{\text{out,on}}+\widehat{P}_{\text{out,off}}$, this ensures equivalence to the convex hull representation.